

Harmonic inversion analysis of exceptional points in resonance spectra

Jacob Fuchs, Jörg Main, Holger Cartarius, Günter Wunner

1. Institut für Theoretische Physik, Universität Stuttgart, 70550 Stuttgart, Germany

Abstract. The spectra of, e.g. open quantum systems are typically given as the superposition of resonances with a Lorentzian line shape, where each resonance is related to a simple pole in the complex energy domain. However, at exceptional points two or more resonances are degenerate and the resulting non-Lorentzian line shapes are related to higher order poles in the complex energy domain. In the Fourier-transform time domain an n -th order exceptional point is characterised by a non-exponentially decaying time signal given as the product of an exponential function and a polynomial of degree $n - 1$. The complex positions and amplitudes of the non-degenerate resonances can be determined with high accuracy by application of the nonlinear harmonic inversion method to the real-valued resonance spectra. We extend the harmonic inversion method to include the analysis of exceptional points. The technique yields, in the energy domain, the amplitudes of the higher order poles contributing to the spectra, and, in the time domain, the coefficients of the polynomial characterising the non-exponential decay of the time signal. The extended harmonic inversion method is demonstrated on two examples, viz. the analysis of exceptional points in resonance spectra of the hydrogen atom in crossed magnetic and electric fields, and an exceptional point occurring in the dynamics of a single particle in a time-dependent harmonic trap.

PACS numbers: 05.70.Jk, 02.30.-f, 32.80.Fb, 31.70.Hq

1. Introduction

Nonlinear methods such as filter diagonalization [1, 2] and harmonic inversion [3–5] have been established which allow for the high-resolution analysis of signals, i.e., the frequencies and amplitudes of a time signal with finite length can be determined with high accuracy without the restriction by the uncertainty principle of the Fourier transform. Those methods can be applied to obtain the eigenspectra of large matrices [6], semiclassical periodic orbit quantisation [7–11], and the analysis of quantum spectra [12, 13]. It is also possible to analyse spectra given as the superposition of resonances with Lorentzian line shape (e.g. the level density or scattering cross section of open quantum systems or microcavities), and to determine the exact positions and corresponding amplitudes of the resonance poles in the complex energy plane [14, 15].

So far, the harmonic inversion method has typically been applied to spectra with non-degenerate complex resonances, and the formulae and derivations presented, e.g. in

[3, 4, 11, 14] are restricted to that case. However, two or more resonances can degenerate at an exceptional point (EP) [16] in the complex energy plane. The occurrence of EPs in open quantum systems has attracted much attention since at these points not only the resonance energies but also the eigenstates coalesce [17–19]. Mathematically, the EPs are branching singularities of non-Hermitian operators [20] and show interesting properties such as the permutation of states when the EP is encircled along a closed path in the parameter space of the system. Theoretical investigations have revealed the existence of EPs, e.g. in spectra of the hydrogen atom in crossed magnetic and electric fields [21, 22] and in Bose-Einstein condensates with long-range interactions [23, 24]. Experimentally, EPs have been observed in spectra of microwave resonators [25–30] and in electronic circuits [31]. Recently, an experiment has been proposed to observe a third order EP in the dynamics of a single particle in a time-dependent harmonic trap [32].

In most of the systems mentioned above signatures of an EP have been verified using properties of the nearly degenerate states in the close vicinity of the exact degeneracy, viz. the permutation behaviour of states when the EP is encircled in the parameter space. However, in some systems, e.g. that discussed by Uzdin *et al* [32], appropriate parameters for the encircling of an EP do not exist or at least are not experimentally accessible. Therefore, alternative methods for the verification of EPs are needed. Dietz *et al* [30] have verified the existence of the EP in a microwave billiard with time-reversal invariance violation both via its encircling and, as an alternative, via directly observing the coalescence of two eigenvectors at the EP. In this paper, we study the features of EPs close to or even exactly at the degeneracy. In resonance spectra a resonance related to an EP is characterised by a non-Lorentzian line shape. In the time domain the survival probability of that resonance shows a non-exponential decay [33, 34]. We extend the harmonic inversion method to handle the degeneracies occurring at EPs. The extended method provides the amplitudes of the first and higher order poles in the complex energy or frequency plane and thus the exact profile of both Lorentzian and non-Lorentzian resonance line shapes. In the time domain the harmonic inversion method yields the decay signal of a resonance given by an exponential function multiplied by a polynomial in time. The observation of a resonance with non-Lorentzian line shape or non-exponentially decaying time signal can be taken as clear evidence for the existence of an exceptional point in the system.

The paper is organised as follows. In section 2 the harmonic inversion method is introduced and extended to the case of degenerate resonances. The method is applied to the analysis of exceptional points by way of two examples in section 3. Firstly, in section 3.1 the non-Lorentzian shape of a resonance related to an EP is revealed in the photoabsorption spectrum of the hydrogen atom in crossed magnetic and electric fields, and, secondly, in section 3.2 a third order EP is observed in the dynamics of a single particle in a time-dependent harmonic trap. Conclusions are drawn in section 4.

2. Harmonic inversion method

For the convenience of the reader we first briefly recapitulate the harmonic inversion method for spectra with non-degenerate resonances and then extend the method by including degeneracies.

2.1. Harmonic inversion of spectra with non-degenerate resonances

A spectrum of non-degenerate resonances is given by the imaginary part of the function

$$G(w) = \sum_k \frac{d_k}{w - w_k}, \quad (1)$$

where the complex parameters w_k with $\text{Im } w_k < 0$ determine the positions and widths of the resonances and the complex d_k describe the amplitudes and details of the Lorentzian line shapes. The aim of the harmonic inversion method is to extract the parameters w_k and d_k from the spectrum given on an equidistant grid of points along the real w -axis.

The first step is to apply the Fourier transform to $G(w)$ to obtain the signal

$$C(s) = \frac{1}{2\pi} \int_{w_-}^{w_+} G(w) \exp(-iws) dw = -i \sum_{k=1}^K d_k \exp(-iw_k s). \quad (2)$$

The parameters w_{\pm} in (2) are introduced to analyse the spectrum in the window $[w_-, w_+]$, i.e. the real parts of the w_k on the r.h.s. of (2) are in the range $w_- < \text{Re } w_k < w_+$. Note that K is the number of poles in that window and can be small compared to the number of poles in the full spectrum $G(w)$. The set of resonances in a larger region is then obtained by analysing several consecutive windows [4]. The harmonic inversion of band-limited signals $C(s)$ with K not larger than about 50 to 200 is numerically more efficient and stable compared to the analysis of a signal with a huge number of frequencies. When the spectrum is given on equidistant grid points $w = w_- + \sigma \Delta w$ for $\sigma = 0, 1, \dots, N-1$ the Fourier integral in (2) is approximated by a discrete sum. Using the time step $\tau = 2\pi/(w_+ - w_-)$ the signal points

$$c_n \equiv C(n\tau) = \frac{\exp(-in\tau w_-)}{2\pi} \sum_{\sigma=0}^{N-1} G(w_- + \sigma \Delta w) \exp\left(-2\pi i \frac{n\sigma}{N}\right) \quad (3)$$

are easily obtained for $n = 0, 1, \dots, N-1$ with a fast Fourier transform (FFT) algorithm. Considering the factor $\exp(-in\tau w_-)$ in (3) as a shift of resonances, $w_k \rightarrow w_k - w_-$, the comparison with the signal $C(s = n\tau)$ in (2) yields

$$c_n \equiv C(n\tau) = \sum_{k=1}^K (-id_k) \{\exp[-i(w_k - w_-)\tau]\}^n = \sum_{k=1}^K \hat{d}_k z_k^n \quad (4)$$

for $n = 0, 1, \dots, N-1$ and with the abbreviations $\hat{d}_k = -id_k$ and $z_k = \exp[-i(w_k - w_-)\tau]$.

The second step is to determine the $2K$ parameters \hat{d}_k and z_k for given signal points c_n . Note that at least $N = 2K$ signal points are required to solve the nonlinear set of equations (4). As the number of frequencies in the band-limited signal is relatively small

($K \sim 50 - 200$) several methods, which otherwise would be numerically unstable, can be applied, e.g. linear predictor, Padé approximant, or direct signal diagonalization [4]. Here, we resort to the Padé approximant. Let us assume for the moment that the signal points c_n are known up to infinity, $n = 0, 1, \dots, \infty$. Interpreting the c_n 's as the coefficients of a Maclaurin series in the variable z^{-1} , we can define the function $g(z) = \sum_{n=0}^{\infty} c_n z^{-n}$. With (4) and the sum rule for geometric series we obtain

$$g(z) \equiv \sum_{n=0}^{\infty} c_n z^{-n} = \sum_{k=1}^K \hat{d}_k \sum_{n=0}^{\infty} (z_k/z)^n = \sum_{k=1}^K \frac{z \hat{d}_k}{z - z_k} \equiv \frac{P_K(z)}{Q_K(z)}. \quad (5)$$

The right-hand side of (5) is a rational function with polynomials of degree K in the numerator and denominator. Evidently, the parameters z_k are the poles of $g(z)$, i.e., the zeros of the polynomial $Q_K(z)$. Of course, the assumption that the coefficients c_n are known up to infinity is not fulfilled and, therefore, the sum over all $c_n z^{-n}$ in (5) cannot be evaluated in practice. However, the convergence of the sum can be accelerated by use of the Padé approximant. Indeed, knowledge of $2K$ signal points c_0, \dots, c_{2K-1} is sufficient for the calculation of the coefficients of the two polynomials

$$P_K(z) = \sum_{k=1}^K b_k z^k \quad \text{and} \quad Q_K(z) = \sum_{k=1}^K a_k z^k - 1. \quad (6)$$

The coefficients a_k with $k = 1, \dots, K$ are obtained as solutions of the linear set of equations

$$c_n = \sum_{k=1}^K a_k c_{n+k}, \quad n = 0, \dots, K-1. \quad (7)$$

Once the a_k are known, the coefficients b_k are given by the explicit formula

$$b_k = \sum_{m=0}^{K-k} a_{k+m} c_m, \quad k = 1, \dots, K. \quad (8)$$

The parameters $z_k = \exp[-i(w_k - w_-)\tau]$ and thus the frequencies

$$w_k = w_- + \frac{i}{\tau} \ln z_k \quad (9)$$

(choosing the branch of the logarithm with $0 \leq \text{Im} \ln z < 2\pi$) are obtained by searching for the zeros of the polynomial $Q_K(z)$ in (6). This is the only nonlinear step of the algorithm. The roots of polynomials can be found, in principle, by application of Laguerre's method [35]. However, it turns out that an alternative method, i.e. the diagonalization of the Hessenberg matrix

$$\mathbf{A} = \begin{pmatrix} -\frac{a_{K-1}}{a_K} & -\frac{a_{K-2}}{a_K} & \dots & -\frac{a_1}{a_K} & \frac{1}{a_K} \\ 1 & 0 & \dots & 0 & 0 \\ 0 & 1 & \dots & 0 & 0 \\ \vdots & & & & \vdots \\ 0 & 0 & \dots & 1 & 0 \end{pmatrix}, \quad (10)$$

with a_k the coefficients of the polynomial $Q_K(z)$ in (6), is a numerically more robust technique for finding the roots of high degree ($K \gtrsim 60$) polynomials [35].

The parameters \hat{d}_k are calculated via the residues of the last two terms of (5). Application of the residue calculus yields

$$\hat{d}_k = -id_k = \frac{P_K(z_k)}{z_k Q'_K(z_k)}, \quad (11)$$

with the prime indicating the derivative d/dz . Note that $Q'_K(z_k)$ vanishes if z_k is a multiple root of the polynomial $Q_K(z)$ and thus equation (11) is not valid for degenerate resonances occurring at exceptional points. In the following we extend the harmonic inversion method to include that case.

2.2. Extension of the harmonic inversion method to degenerate resonances

Degenerate resonances cannot be described by simple poles of the function $G(w)$ but higher order poles are required. Therefore, the ansatz (1) is generalised to

$$G(w) = \sum_k \sum_{\alpha=1}^{r_k} \frac{d_{k,\alpha}}{(w - w_k)^\alpha}, \quad (12)$$

where r_k is the order of degeneracy of resonance k . Note that resonances with $r_k > 1$ in spectra given as $\text{Im } G(w)$ have a non-Lorentzian line shape. The aim is now to extract the complex resonance positions w_k and amplitudes $d_{k,\alpha}$ from a given spectrum.

The first step is again the computation of a band-limited time signal by a windowed Fourier transform of $G(w)$. Writing $G(w)$ in (12) as

$$G(w) = \sum_k \sum_{\alpha=1}^{r_k} d_{k,\alpha} \frac{(-1)^{\alpha-1}}{(\alpha-1)!} \left(\frac{d}{dw}\right)^{\alpha-1} (w - w_k)^{-1}$$

we obtain

$$\begin{aligned} C(s) &= \frac{1}{2\pi} \int_{w_-}^{w_+} G(w) \exp(-iws) dw \\ &= \sum_k \sum_{\alpha=1}^{r_k} d_{k,\alpha} \frac{(-1)^{\alpha-1}}{(\alpha-1)!} (is)^{\alpha-1} (-i) \exp(-iw_k s), \end{aligned} \quad (13)$$

where the sum over k is now restricted to those resonances with $\text{Re } w_k \in [w_-, w_+]$. At discrete grid points $s = n\tau$ (with $n = 0, 1, \dots, N-1$) the signal reads

$$c_n \equiv C(n\tau) = \sum_k \sum_{\alpha=1}^{r_k} (-id_{k,\alpha}) \frac{(-in\tau)^{\alpha-1}}{(\alpha-1)!} \exp[-i(w_k - w_-)n\tau]. \quad (14)$$

With the abbreviations

$$\hat{d}_{k,\alpha} = -id_{k,\alpha} \frac{(-i\tau)^{\alpha-1}}{(\alpha-1)!} \quad \text{and} \quad z_k = \exp[-i(w_k - w_-)\tau] \quad (15)$$

we finally obtain the nonlinear set of equations

$$c_n = \sum_k \sum_{\alpha=1}^{r_k} \hat{d}_{k,\alpha} n^{\alpha-1} z_k^n, \quad n = 0, 1, \dots, 2K-1, \quad (16)$$

Table 1. Stirling numbers of the second kind $\mathcal{S}(n, k)$ for $n, k \leq 5$.

	k					
$\mathcal{S}(n, k)$	0	1	2	3	4	5
$n = 0$	1					
$n = 1$	0	1				
$n = 2$	0	1	1			
$n = 3$	0	1	3	1		
$n = 4$	0	1	17	6	1	
$n = 5$	0	1	15	25	10	1

where $K = \sum_k r_k$ is the total number of resonances of the band-limited signal counting all multiplicities.

The second step, i.e. the solution of the nonlinear set of equations (16), also starts analogously to the non-degenerate case. Interpreting the c_n 's in (16) as the coefficients of a Maclaurin series in z^{-1} given for $n = 0, 1, \dots, \infty$ we now obtain

$$g(z) \equiv \sum_{n=0}^{\infty} c_n z^{-n} = \sum_k \sum_{\alpha=1}^{r_k} \hat{d}_{k,\alpha} \sum_{n=0}^{\infty} n^{\alpha-1} (z_k/z)^n \equiv \frac{P_K(z)}{Q_K(z)}. \quad (17)$$

The rational function with the polynomials $P_K(z)$ and $Q_K(z)$ on the r.h.s. of (17) is obtained in the same way as in (5) using equations (6)-(8). The parameters z_k are the roots of the polynomial $Q_K(z)$, however, the difference to the non-degenerate case is that now each root z_k is r_k -fold degenerate. For $\alpha > 1$ the sum on the l.h.s. of (17) is no longer a simple geometric series. In the following we use the relation (see appendix)

$$\sum_{n=0}^{\infty} n^{\alpha-1} x^n = \sum_{n=0}^{\alpha-1} n! \mathcal{S}(\alpha-1, n) \frac{x^n}{(1-x)^{n+1}} = \frac{x^\alpha f_\alpha(x)}{(x-1)^\alpha} \quad (18)$$

with

$$\mathcal{S}(n, k) = \frac{1}{k!} \sum_{\mu=0}^k (-1)^{k-\mu} \binom{k}{\mu} \mu^n \quad (19)$$

the Stirling numbers of the second kind [36], and the functions

$$f_\alpha(x) = (-1)^\alpha \sum_{\nu=0}^{\alpha-1} \nu! \mathcal{S}(\alpha-1, \nu) \frac{1}{x} \left(\frac{1-x}{x} \right)^{\alpha-1-\nu}. \quad (20)$$

A few Stirling numbers $\mathcal{S}(n, k)$ for $n, k \leq 5$ are given in table 1. Using the second term of (18) the function $g(z)$ can be written as

$$g(z) = \sum_k \sum_{\alpha=1}^{r_k} \hat{d}_{k,\alpha} \sum_{n=0}^{\alpha-1} n! \mathcal{S}(\alpha-1, n) \frac{z z_k^n}{(z - z_k)^{n+1}} \equiv \frac{P_K(z)}{Q_K(z)}. \quad (21)$$

Both sides of (21) are rational functions in z with degree K polynomials in the numerator and denominator. Using a partial fraction decomposition of $P_K(z)/[zQ_K(z)]$ the parameters $\hat{d}_{k,\alpha}$ can, in principle, be obtained as solutions of sets of linear equations

comparing the coefficients of terms $(z - z_k)^{-n}$ with the same root z_k and order n . However, it is also possible to derive explicit formulae for the computation of the $\hat{d}_{k,\alpha}$ [37]. Using the last term of (18) equation (21) can also be written as (we drop the subscript K on the polynomials $P(z)$ and $Q(z)$ in the following)

$$g(z) = \sum_k \sum_{\alpha=1}^{r_k} \hat{d}_{k,\alpha} \frac{f_{k,\alpha}(z)}{(1 - z/z_k)^\alpha} \equiv \frac{P(z)}{Q(z)} \quad (22)$$

with the functions $f_{k,\alpha}(z) = f_\alpha(z_k/z)$, which are polynomials of degree α in z . Equation (22) is now multiplied with $Q(z)$, and both sides are expanded, for each root z_k , in a Taylor series of degree $r_k - 1$ around $z = z_k$. Comparison of the coefficients of terms $(z - z_k)^l$ for $l = 0, \dots, r_k - 1$ yields

$$\sum_{\alpha=r_k-l}^{r_k} \hat{d}_{k,\alpha} \sum_{\nu=0}^{l+\alpha-r_k} (r_k + \nu - l - 1)! \mathcal{S}(\alpha, r_k + \nu - l) z_k^{r_k+\nu-l} Q^{[r_k+\nu]}(z_k) = P^{[l]}(z_k) \quad (23)$$

with the notation

$$f^{[n]}(x) = \frac{1}{n!} f^{(n)}(x) = \frac{1}{n!} \left(\frac{d}{dz} \right)^n f(z) \Big|_{z=x} . \quad (24)$$

From (23) we finally obtain

$$\hat{d}_{k,\alpha} = \frac{P^{[r_k-\alpha]}(z_k)}{(\alpha-1)! z_k^\alpha Q^{[r_k]}(z_k)} - \sum_{\mu=\alpha+1}^{r_k} \hat{d}_{k,\mu} \sum_{\nu=0}^{\mu-\alpha} \frac{(\alpha-1+\nu)! \mathcal{S}(\mu, \alpha+\nu) z_k^\nu Q^{[r_k+\nu]}(z_k)}{(\alpha-1)! Q^{[r_k]}(z_k)} . \quad (25)$$

For every index k equation (25) can be evaluated recursively starting with the highest value $\alpha = r_k$ down to $\alpha = 1$. In the following some special cases of (25) are given explicitly. For a non-degenerate resonance ($r_k = 1$) we obtain the already known formula

$$\hat{d}_{k,1} = \frac{P(z_k)}{z_k Q^{[1]}(z_k)} = \frac{P(z_k)}{z_k Q^{(1)}(z_k)} . \quad (26)$$

For a twofold degenerate resonance ($r_k = 2$) equation (25) yields

$$\begin{aligned} \hat{d}_{k,2} &= \frac{P(z_k)}{z_k^2 Q^{[2]}(z_k)} = \frac{2P(z_k)}{z_k^2 Q^{(2)}(z_k)} , \\ \hat{d}_{k,1} &= \frac{P^{[1]}(z_k)}{z_k Q^{[2]}(z_k)} - \hat{d}_{k,2} \left(1 + \frac{z_k Q^{[3]}(z_k)}{Q^{[2]}(z_k)} \right) = \frac{2P^{(1)}(z_k)}{z_k Q^{(2)}(z_k)} - \hat{d}_{k,2} \left(1 + \frac{z_k Q^{(3)}(z_k)}{3Q^{(2)}(z_k)} \right) . \end{aligned} \quad (27)$$

Threefold degenerate resonances will probably occur more rarely. For $r_k = 3$ the amplitudes read:

$$\begin{aligned} \hat{d}_{k,3} &= \frac{P(z_k)}{2z_k^3 Q^{[3]}(z_k)} = \frac{3P(z_k)}{z_k^3 Q^{(3)}(z_k)} , \\ \hat{d}_{k,2} &= \frac{P^{[1]}(z_k)}{z_k^2 Q^{[3]}(z_k)} - \hat{d}_{k,3} \left(3 + \frac{2z_k Q^{[4]}(z_k)}{Q^{[3]}(z_k)} \right) = \frac{6P^{(1)}(z_k)}{z_k^2 Q^{(3)}(z_k)} - \hat{d}_{k,3} \left(3 + \frac{z_k Q^{(4)}(z_k)}{2Q^{(3)}(z_k)} \right) , \\ \hat{d}_{k,1} &= \frac{P^{[2]}(z_k)}{z_k Q^{[3]}(z_k)} - \hat{d}_{k,2} \left(1 + \frac{z_k Q^{[4]}(z_k)}{Q^{[3]}(z_k)} \right) - \hat{d}_{k,3} \left(1 + \frac{3z_k Q^{[4]}(z_k)}{Q^{[3]}(z_k)} + \frac{2z_k^2 Q^{[5]}(z_k)}{Q^{[3]}(z_k)} \right) \\ &= \frac{3P^{(2)}(z_k)}{z_k Q^{(3)}(z_k)} - \hat{d}_{k,2} \left(1 + \frac{z_k Q^{(4)}(z_k)}{4Q^{(3)}(z_k)} \right) - \hat{d}_{k,3} \left(1 + \frac{3z_k Q^{(4)}(z_k)}{4Q^{(3)}(z_k)} + \frac{z_k^2 Q^{(5)}(z_k)}{10Q^{(3)}(z_k)} \right) . \end{aligned} \quad (28)$$

The parameters z_k and r_k are the roots and corresponding multiplicities of the polynomial $Q(z)$. The values of the w_k and $d_{k,\alpha}$ in (12) are finally obtained by using (9) for the frequencies and

$$d_{k,\alpha} = i \hat{d}_{k,\alpha} \frac{(\alpha - 1)!}{(-i\tau)^{\alpha-1}} \quad (29)$$

for the amplitudes.

In practical applications of the harmonic inversion method the roots z_k of the polynomial $Q(z)$ can again be computed by e.g. Laguerre's method or diagonalization of the Hessenberg matrix (10). Numerically two or more roots will typically not coincide exactly, however, the distance between neighbouring roots can become very small. In that case, the application of formulae for the degenerate case derived in this section is meaningful. Close to a degeneracy related to an exceptional point the amplitudes d_k in (1) of the non-degenerate resonances can become very large and diverge at the exact EP [22]. By contrast, the amplitudes $d_{k,\alpha}$ in (12) of higher order poles describing the non-Lorentzian shape of a resonance close to an EP only weakly depend on the distances between nearly degenerate z_k values, as will be shown in section 3. In an implementation of the extended harmonic inversion method it is useful to introduce a parameter δ and to assume z_k values with distances less than δ to be degenerate. The formulae for the amplitudes of a degenerate resonance require inserting the parameter z_k of the degenerate frequency. In the numerical procedure that z_k value is taken as the geometric mean of the individual nearly degenerate z_k 's.

3. Analysis of exceptional points

We now present applications of the extended harmonic inversion method for the analysis of exceptional points. In section 3.1 we analyse photoabsorption spectra of the hydrogen atom in crossed magnetic and electric fields, and in section 3.2 we investigate the occurrence of an EP in the dynamics of a single particle in a time-dependent harmonic trap.

3.1. Hydrogen atom in crossed magnetic and electric fields

Atoms in crossed static magnetic and electric fields are open quantum systems, which have been investigated in detail both experimentally [38–41] and theoretically [42–45]. For the hydrogen atom in crossed fields the Hamiltonian [in atomic units with $\gamma = B/(2.35 \times 10^5 \text{ T})$, $f = F/(5.14 \times 10^{11} \text{ V/m})$, and L_z the z -component of the angular momentum] reads

$$H = \frac{1}{2} \mathbf{p}^2 - \frac{1}{r} + \frac{1}{2} \gamma L_z + \frac{1}{8} \gamma^2 (x^2 + y^2) + fx. \quad (30)$$

As the crossed fields hydrogen atom is an open system the photoabsorption spectrum is a superposition of resonances with nonzero line widths. The photoabsorption cross

section for excitations of an initial state ψ_0 at energy E_0 to a final state at energy E can be written as [46]

$$\sigma(E) = 4\pi\alpha(E - E_0) \operatorname{Im} \left(\sum_j \frac{\langle \psi_0 | D | \psi_j \rangle^2}{E_j - E} \right), \quad (31)$$

with α the fine-structure constant and D the dipole operator. The E_j are complex energy eigenvalues and the ψ_j the corresponding complex eigenstates, which can be computed with the complex coordinate rotation method [47–49].

The resonance positions in the complex energy plane depend on two parameters, viz. the magnetic and electric field strengths γ and f . By varying the two field strengths it can happen that two resonances coincide at the same complex energy. Various methods can be applied to investigate whether or not the degeneracy is an exceptional point. The most established technique is to encircle the critical point in the (γ, f) parameter space [21, 22]. The EP is a branching singularity characterised by the property that the two states permute when the EP is encircled along a closed path. The method, however, requires the analysis of a sufficiently high number of measured or computed photoabsorption spectra at (γ, f) parameters surrounding the critical point. An alternative method is to analyse a degenerate or nearly degenerate resonance with the extended harmonic inversion method. Here, the fingerprint of an EP is a non-Lorentzian line shape of the resonance caused by higher order poles ($\alpha \geq 2$) in the ansatz (12). The advantage of the method is that a single spectrum is sufficient to reveal exceptional points.

As an example we analyse the resonance at energy $E \approx -0.0221$ in the photoabsorption spectrum of the crossed fields hydrogen atom at the field strengths $\gamma = 0.004604$ and $f = 0.0002177$ shown as solid black line in figure 1. The photoabsorption cross section $\sigma(E)$ is computed for transitions from the initial state $|2p0\rangle$ to final states with light polarised parallel to the magnetic field axis as described in [22]. The harmonic inversion analysis of the numerically exact spectrum reveals two nearly degenerate complex energies E_1 and E_2 shown in the lower panel of figure 1. They are related to the exceptional point labelled 8 in table I of [22]. The values of the energies and amplitudes obtained by the harmonic inversion method are presented in table 2. As the complex energies E_1 and E_2 do not exactly coincide the two corresponding amplitudes d_1 and d_2 can be computed with equation (26) valid for non-degenerate resonances. However, it should be noted that roughly $d_2 \approx -d_1$, i.e. both amplitudes cancel each other to a large amount. The values of d_1 and d_2 strongly depend on the distance between the two nearly degenerate resonances and diverge at the exact EP where $E_1 = E_2$. It is therefore more appropriate to describe the resonance in figure 1 using the ansatz (12) for a non-Lorentzian line shape. The amplitudes $d_{1,1}$ and $d_{1,2}$ in table 2 have been computed with (27) for a twofold degenerate resonance at the mean energy $\bar{E}_1 = (E_1 + E_2)/2$. The Lorentzian part of the resonance related to a first order pole in (12) and the non-Lorentzian part related to a second order pole in (12) are shown as grey dashed and blue dotted line in figure 1, respectively, and the sum of the two

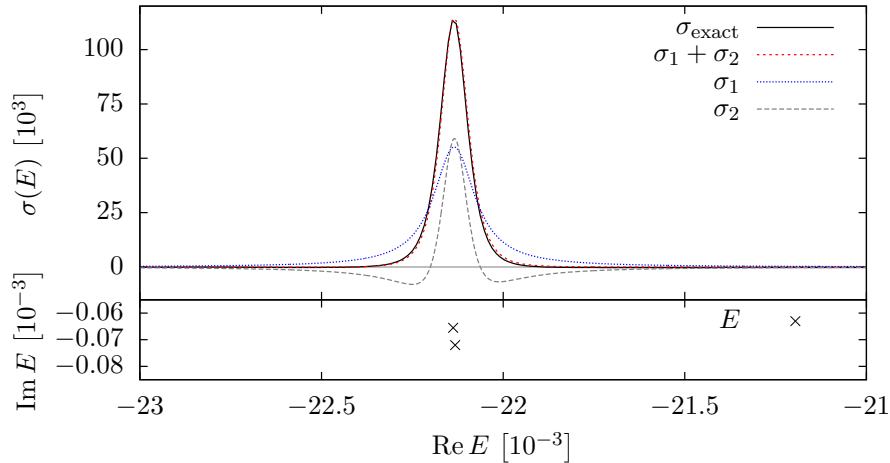


Figure 1. Photoabsorption spectrum around the nearly degenerate resonance at $E \approx -0.0221$ of the crossed fields hydrogen atom at field strengths $\gamma = 0.004604$ and $f = 0.0002177$. The numerically exact cross section σ_{exact} (black solid line) is excellently reproduced by the sum $\sigma_1 + \sigma_2$ (red dashed line) of the contributions σ_1 related to a first order pole (blue dotted line) and σ_2 related to a second order pole (grey dashed line). The non-vanishing contribution of the second order pole clearly indicates that the resonance is related to an exceptional point. The positions E_1 and E_2 of the two nearly degenerate resonance poles are marked in the lower panel. All values are in atomic units.

Table 2. Harmonic inversion analysis of the degenerate resonance at $E \approx -0.0221$ in figure 1. The amplitudes d_1 and d_2 have been obtained with (26) for the two slightly different complex energies E_1 and E_2 . The amplitudes $d_{1,1}$ and $d_{1,2}$ have been computed with (27) for a twofold degenerate resonance at the mean energy $\bar{E}_1 = (E_1 + E_2)/2$.

	$\text{Re } E$	$\text{Im } E$		$\text{Re } d$	$\text{Im } d$
E_1	-0.0221376	-0.0000655	d_1	10.034060	14.122197
E_2	-0.0221322	-0.0000720	d_2	-10.029165	-12.224046
\bar{E}_1	-0.0221349	-0.0000688	$d_{1,1}$	0.004687	1.897540
			$d_{1,2}$	-0.000140	-0.000006

contributions (red dashed line) reproduces the total photoabsorption cross section (black solid line) very well. The amplitudes $d_{1,1}$ and $d_{1,2}$ only weakly depend on how closely the exact EP is approached and, in particular, do not diverge at the EP. This clearly demonstrates that the extended harmonic inversion method introduced in section 2.2 is not restricted to the case of exact degeneracies but is well suited even for the analysis of nearly degenerate resonances. Furthermore, the method allows for the detection of an EP using a single spectrum. The contributions of both the first and second order pole in figure 1 are of similar size. The non-vanishing contribution of the second order pole provides clear evidence that the two resonance poles in the lower panel of figure 1 are

related to a second order exceptional point. By contrast, the method of encircling the EP requires several spectra at various parameter values to observe the permutation of states as a fingerprint of the EP [21, 22].

The spectrum in figure 1 has been computed numerically, however, it is important to note that high-resolution spectroscopy of atoms in external fields allows for the experimental observation of exceptional points. The resolution of the experiment must be sufficiently high to resolve the line shapes of resonances and, in particular, to distinguish between Lorentzian and non-Lorentzian profiles. The harmonic inversion analysis of experimental high-resolution spectra is an alternative to the measurement of the survival probability $S(t) = |\langle \psi(0) | \psi(t) \rangle|^2$ of a decaying degenerate resonance $\psi(t)$, which has been excited with a laser whose bandwidth is large compared to the width of the resonance [34]. Nevertheless, the extended harmonic inversion method can also be applied to adjust the measured survival probability to the functional form of the signal (13), and to detect, e.g., a second order EP by the non-exponential decay of the survival probability $S(t) = |1 - at|^2 \exp(2\text{Im } E_{\text{EP}}t/\hbar)$ with a parameter $a \neq 0$.

3.2. Single particle in a time-dependent harmonic trap

As a second example for the application of the extended harmonic inversion method we study the dynamics of a single particle with mass m in a harmonic oscillator with changing frequency given by the Hamiltonian

$$H = \frac{p^2}{2m} + \frac{m}{2}\omega^2(t)x^2. \quad (32)$$

It has been shown by Uzdin *et al* [32] that when the frequency is changed by keeping the dimensionless adiabatic parameter

$$\mu = \left[\frac{1}{\omega^2(t)} \right] \frac{d\omega(t)}{dt} \quad (33)$$

fixed, the time evolution features an exceptional point at $\mu = 2$. The variance of the position operator $\langle x^2 \rangle$ normalised by the width of the instantaneous potential $1/\sqrt{2m\omega(t)}$ as function of the renormalised time $s = (1/\mu) \ln[\omega(t)/\omega(0)]$ is given by the signal

$$C(s) = \frac{\mu^2 \cosh(s\sqrt{\mu^2 - 4}/\mu) + \mu\sqrt{\mu^2 - 4} \sinh(s\sqrt{\mu^2 - 4}/\mu) - 4}{\mu^2 - 4} \quad (34)$$

and illustrated for various values of μ in figure 2. The signal $C(s)$ shows a sharp transition from an oscillatory to a monotonic exponential dynamics at $\mu = 2$, where three frequencies of the signal are identical. Is this degeneracy a third order EP? That question cannot be answered with the established method of observing the permutation of the frequencies when the EP is encircled in the parameter space because the single control parameter μ of the system does not allow for such an encircling. Uzdin *et al* [32] propose to observe the third order derivative of the renormalised variance which should vanish at $\mu = 2$, where $C(s)$ is a second order polynomial in s . However, higher order derivatives of the experimentally measured signal may strongly suffer from noise.

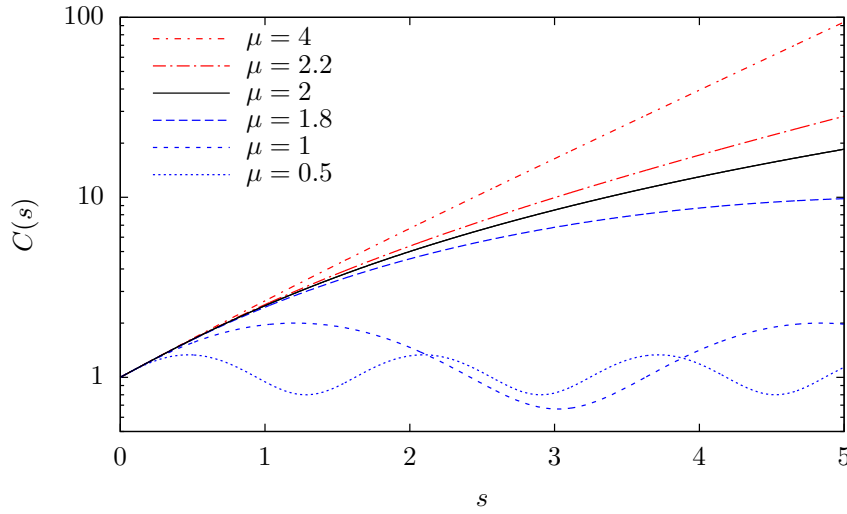


Figure 2. Signal $C(s)$ obtained as normalised variance of the position operator $\langle x^2 \rangle$ as a function of renormalised time of a particle in a time-dependent harmonic trap for various values of the adiabatic parameter μ . A transition from an oscillatory to a monotonically growing exponential dynamics occurs at $\mu = 2$.

As an alternative approach we suggest to use the extended harmonic inversion method to identify the EP unambiguously. For the analysis of signals it is convenient to write the signal $C(s)$ defined in (13) in the form

$$C(s) = \sum_k \sum_{\alpha=1}^{r_k} \tilde{d}_{k,\alpha} s^{\alpha-1} \exp(-i w_k s) \quad (35)$$

with

$$\tilde{d}_{k,\alpha} = \frac{(-i)^\alpha}{(\alpha-1)!} d_{k,\alpha}, \quad (36)$$

and to determine the frequencies w_k and amplitudes $\tilde{d}_{k,\alpha}$ with the extended harmonic inversion method. The results for the analysis of the signal (34) are presented in figure 3. The numerical procedure reveals that the signal possesses exactly three frequencies with nonzero amplitudes. The frequencies are shown in figure 3(a). Evidently, $w_1 = 0$ is constant and w_2 and w_3 undergo a transition from purely real to purely imaginary frequencies at $\mu = 2$, which is directly related to the transition from an oscillatory to a monotonic exponential dynamics in figure 2. The amplitudes \tilde{d}_1 to \tilde{d}_3 in figure 3(b) obtained with equation (26) for non-degenerate resonances diverge at $\mu = 2$, where the three frequencies coincide. By contrast, the amplitudes $\tilde{d}_{1,1}$ to $\tilde{d}_{1,3}$ in figure 3(c) obtained with equation (28) for a threefold degenerate resonance are smooth functions around $\mu = 2$. The nonzero value $\tilde{d}_{1,3} = 0.5$ in the region $\mu \approx 2$ provides clear evidence, that the critical point is a third-order EP.

In any realisation of the experiment proposed by Uzdin *et al* [32] the frequency $\omega(t)$ of the time-dependent harmonic trap can certainly be varied only within a limited finite range, and thus the signal $C(s)$ in figure 2 cannot be measured at large values s

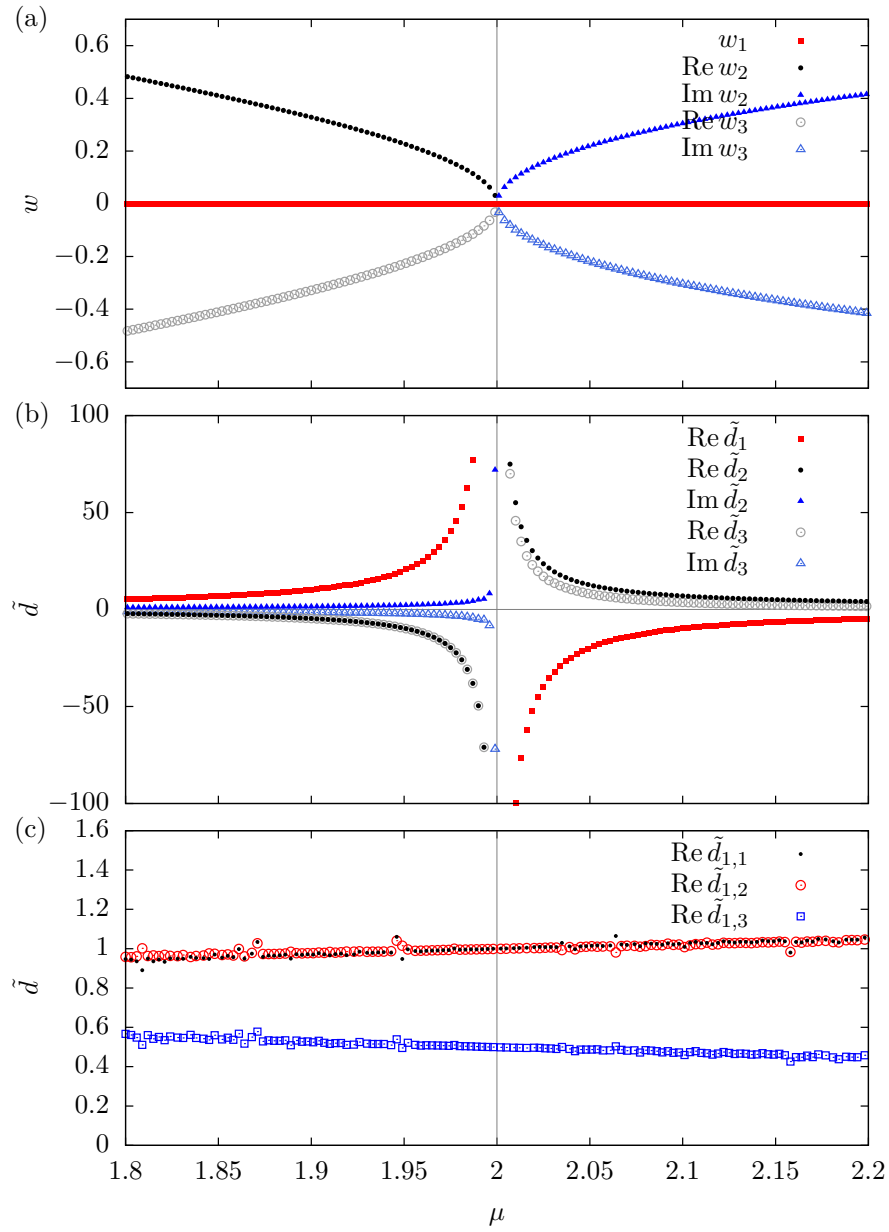


Figure 3. (a) Frequencies and (b), (c) amplitudes obtained by the harmonic inversion analysis of the signal $C(s)$ in (34) as functions of the adiabatic parameter μ . The amplitudes \tilde{d}_1 to \tilde{d}_3 in (b) obtained with equation (26) for non-degenerate resonances diverge at $\mu = 2$, where the three frequencies in (a) coincide. By contrast, the amplitudes $\tilde{d}_{1,1}$ to $\tilde{d}_{1,3}$ in (c) obtained with equation (28) for a threefold degenerate resonance are smooth functions around $\mu = 2$. The nonzero value $\tilde{d}_{1,3} = 1$ in the region $\mu \approx 2$ provides clear evidence, that the critical point is a third-order EP.

of the renormalised time. The results in figure 3 have been obtained by analysing the region $s \in [0, 2]$ of the signal. Note that at small values of s the signals belonging to different parameters μ become more and more similar (see, e.g. the signals with $\mu = 1.8$, $\mu = 2$, and $\mu = 2.2$ in figure 2) and thus the extraction of the correct frequencies and amplitudes from a short signal is a nontrivial task. We have checked that signals with a short signal length down to $s_{\max} \approx 1$ are sufficient to clearly observe the degeneracy of the three frequencies at $\mu = 2$ and to verify the nonzero amplitude $\tilde{d}_{1,3} \approx 0.5$ indicating the third-order EP. Furthermore, the harmonic inversion method is robust against a certain amount of noise in the signal [4, 5]. For these reasons the extended harmonic inversion method introduced in this paper is ideally suited to reveal exceptional points in experimentally measured signals.

4. Conclusion

We have extended the harmonic inversion method to allow for the analysis of spectra and time signals with degeneracies. In the energy or frequency domain the parameters of non-Lorentzian line shapes related to higher order resonance poles and in the time domain the parameters of non-exponentially decaying contributions to time signals can be extracted. The method has been applied to reveal exceptional points in the photoabsorption spectrum of the hydrogen atom in crossed electric and magnetic fields and in the dynamics of a single particle in a time-dependent harmonic trap. The harmonic inversion analysis is an alternative to the observation of the permutation of states when the exceptional point is encircled in the parameter space. The advantage of the method is that it allows for the verification of an EP even in cases when appropriate parameters for the encircling of the EP are not available. In the future the extended harmonic inversion method can be used to observe exceptional points in a large variety of physical systems, including e.g. electronic circuits, mechanical systems, atomic spectra, Bose-Einstein condensates, microcavities, and microwave resonators. In particular it will be interesting to use the method for the identification of exceptional points in systems in which they could be applied to manipulate the system. For example, exceptional points are discussed in molecular physics to prepare molecules in a defined vibrational level [50, 51]. In [30] the EP distinguishes between the PT-symmetric and the PT-broken phase, and in [32] it is shown that an EP can be used to shift an oscillator to an exponential decaying regime.

Appendix A. Derivation of the sum relation

Here we present derivations of equations (18) and (20) for the series $\sum_{n=0}^{\infty} n^{\alpha-1} x^n$. We start with the formula

$$\left(x \frac{d}{dx}\right)^{\alpha} f(x) = \sum_{n=0}^{\alpha} \mathcal{S}(\alpha, n) x^n \left(\frac{d}{dx}\right)^n f(x) \quad (\text{A.1})$$

which can easily be proved by induction: With the Stirling numbers $\mathcal{S}(\alpha, \alpha + 1) = 0$ and $\mathcal{S}(\alpha, -1) = 0$ we obtain

$$\begin{aligned} \left(x \frac{d}{dx}\right)^{\alpha+1} f(x) &= \sum_{n=0}^{\alpha} \mathcal{S}(\alpha, n) \left(n x^n \left(\frac{d}{dx}\right)^n f(x) + x^{n+1} \left(\frac{d}{dx}\right)^{n+1} f(x) \right) \\ &= \sum_{n=0}^{\alpha+1} (n \mathcal{S}(\alpha, n) + \mathcal{S}(\alpha, n-1)) x^n \left(\frac{d}{dx}\right)^n f(x), \end{aligned} \quad (\text{A.2})$$

with an index shift $n \rightarrow n-1$ in the second term of the upper equation. Using the recurrence relation $\mathcal{S}(\alpha+1, n) = n \mathcal{S}(\alpha, n) + \mathcal{S}(\alpha, n-1)$ [36] we obtain (A.1).

Now this formula is applied to the geometric series. On the one hand we have

$$\left(x \frac{d}{dx}\right)^{\alpha-1} \sum_{n=0}^{\infty} x^n = \left(x \frac{d}{dx}\right)^{\alpha-1} \frac{1}{1-x} = \sum_{n=0}^{\alpha-1} n! \mathcal{S}(\alpha-1, n) \frac{x^n}{(1-x)^{n+1}}. \quad (\text{A.3})$$

On the other hand, the derivatives of the geometric series yield

$$\left(x \frac{d}{dx}\right)^{\alpha-1} \sum_{n=0}^{\infty} x^n = \sum_{n=0}^{\infty} n^{\alpha-1} x^n, \quad (\text{A.4})$$

and therefore we arrive at equation (18). To obtain the functions $f_{\alpha}(x)$ in (18) we factorise the highest powers of x and $1/(1-x)$

$$\sum_{n=0}^{\infty} n^{\alpha-1} x^n = \frac{x^{\alpha}}{(1-x)^{\alpha}} \sum_{n=0}^{\alpha-1} n! \mathcal{S}(\alpha-1, n) \left(\frac{1}{x}\right) \left(\frac{1-x}{x}\right)^{\alpha-n-1}, \quad (\text{A.5})$$

which yields (20).

References

- [1] M. R. Wall and D. Neuhauser. Extraction, through filter-diagonalization, of general quantum eigenvalues or classical normal mode frequencies from a small number of residues or a short-time segment of a signal. I. Theory and application to a quantum-dynamics model. *J. Chem. Phys.*, 102:8011–8022, 1995.
- [2] V. A. Mandelshtam and H. S. Taylor. Spectral analysis of time correlation function for a dissipative dynamical system using filter diagonalization: Application to calculation of unimolecular decay rates. *Phys. Rev. Lett.*, 78:3274–3277, 1997.
- [3] V. A. Mandelshtam and H. S. Taylor. Harmonic inversion of time signals and its applications. *J. Chem. Phys.*, 107:6756–6769, 1997.
- [4] Dž. Belkić, P. A. Dando, J. Main, and H. S. Taylor. Three novel high-resolution nonlinear methods for fast signal processing. *J. Chem. Phys.*, 113:6542–6556, 2000.
- [5] Dž. Belkić, P. A. Dando, J. Main, H. S. Taylor, and S. K. Shin. Decimated signal diagonalization for Fourier transform spectroscopy. *J. Phys. Chem. A*, 104:11677–11684, 2000.
- [6] Dž. Belkić, P. A. Dando, H. S. Taylor, and J. Main. Decimated signal diagonalization for obtaining the complete eigenspectra of large matrices. *Chem. Phys. Lett.*, 315:135–139, 1999.
- [7] J. Main, V. A. Mandelshtam, and H. S. Taylor. Periodic orbit quantization by harmonic inversion of Gutzwiller’s recurrence function. *Phys. Rev. Lett.*, 79:825–828, 1997.
- [8] J. Main, V. A. Mandelshtam, G. Wunner, and H. S. Taylor. Harmonic inversion as a general method for periodic orbit quantization. *Nonlinearity*, 11:1015–1035, 1998.
- [9] J. Main and G. Wunner. Periodic orbit quantization of mixed regular-chaotic systems. *Phys. Rev. Lett.*, 82:3038–3041, 1999.

- [10] J. Main and G. Wunner. Semiclassical calculation of transition matrix elements for atoms in external fields. *Phys. Rev. A*, 59:R2548–R2551, 1999.
- [11] J. Main, P. A. Dando, Dž. Belkić, and H. S. Taylor. Decimation and harmonic inversion of periodic orbit signals. *J. Phys. A*, 33:1247–1263, 2000.
- [12] J. Main, V. A. Mandelshtam, and H. S. Taylor. High resolution quantum recurrence spectra: Beyond the uncertainty principle. *Phys. Rev. Lett.*, 78:4351–4354, 1997.
- [13] J. Main. Use of harmonic inversion techniques in semiclassical quantization and analysis of quantum spectra. *Phys. Rep.*, 316:233–338, 1999.
- [14] J. Wiersig and J. Main. Fractal Weyl law for chaotic microcavities: Fresnel’s laws imply multifractal scattering. *Phys. Rev. E*, 77:036205, 2008.
- [15] H. Schomerus, J. Wiersig, and J. Main. Lifetime statistics in chaotic dielectric microresonators. *Phys. Rev. A*, 79:053806, 2009.
- [16] T. Kato. *Perturbation Theory of Linear Operators*. Springer, Berlin, 1966.
- [17] W. D. Heiss and A. L. Sannino. Avoided level crossings and exceptional points. *J. Phys. A*, 23:1167–1178, 1990.
- [18] W. D. Heiss. Chirality of wavefunctions for three coalescing levels. *J. Phys. A: Math. Theor.*, 41:244010, 2008.
- [19] W. D. Heiss. The physics of exceptional points. *J. Phys. A: Math. Theor.*, 45:444016, 2012.
- [20] N. Moiseyev. *Non-Hermitian Quantum Mechanics*. Cambridge University Press, Cambridge, 2011.
- [21] H. Cartarius, J. Main, and G. Wunner. Exceptional points in atomic spectra. *Phys. Rev. Lett.*, 99:173003, 2007.
- [22] H. Cartarius, J. Main, and G. Wunner. Exceptional points in the spectra of atoms in external fields. *Phys. Rev. A*, 79:053408, 2009.
- [23] H. Cartarius, J. Main, and G. Wunner. Discovery of exceptional points in the Bose-Einstein condensation of gases with attractive $1/r$ interaction. *Phys. Rev. A*, 77:013618, 2008.
- [24] R. Gutöhrlein, J. Main, H. Cartarius, and G. Wunner. Bifurcations and exceptional points in dipolar Bose-Einstein condensates. *J. Phys. A: Math. Theor.*, 46:305001, 2013.
- [25] M. Philipp, P. von Brentano, G. Pascovici, and A. Richter. Frequency and width crossing of two interacting resonances in a microwave cavity. *Phys. Rev. E*, 62:1922–1926, 2000.
- [26] C. Dembowski, H.-D. Gräf, H. L. Harney, A. Heine, W. D. Heiss, H. Rehfeld, and A. Richter. Experimental observation of the topological structure of exceptional points. *Phys. Rev. Lett.*, 86:787–790, 2001.
- [27] C. Dembowski, B. Dietz, H.-D. Gräf, H. L. Harney, A. Heine, W. D. Heiss, and A. Richter. Observation of a chiral state in a microwave cavity. *Phys. Rev. Lett.*, 90:034101, 2003.
- [28] C. Dembowski, B. Dietz, H.-D. Gräf, H. L. Harney, A. Heine, W. D. Heiss, and A. Richter. Encircling an exceptional point. *Phys. Rev. E*, 69:056216, 2004.
- [29] B. Dietz, T. Friedrich, J. Metz, M. Miski-Oglu, A. Richter, F. Schäfer, and C. A. Stafford. Rabi oscillations at exceptional points in microwave billiards. *Phys. Rev. E*, 75:027201, 2007.
- [30] B. Dietz, H. L. Harney, O. N. Kirillov, M. Miski-Oglu, A. Richter, and F. Schäfer. Exceptional points in a microwave billiard with time-reversal invariance violation. *Phys. Rev. Lett.*, 106:150403, 2011.
- [31] T. Stehmann, W. D. Heiss, and F. G. Scholtz. Observation of exceptional points in electronic circuits. *J. Phys. A: Math. Gen.*, 37:7813, 2004.
- [32] R. Uzdin, E. G. Dalla Torre, R. Kosloff, and N. Moiseyev. Effects of an exceptional point on the dynamics of a single particle in a time-dependent harmonic trap. *Phys. Rev. A*, 88:022505, 2013.
- [33] W. D. Heiss. Time behaviour near to spectral singularities. *Eur. Phys. J. D*, 60:257–261, 2010.
- [34] H. Cartarius and N. Moiseyev. Fingerprints of exceptional points in the survival probability of resonances in atomic spectra. *Phys. Rev. A*, 84:013419, 2011.
- [35] W. H. Press, S. A. Teukolsky, W. T. Vetterling, and B. P. Flannery. *Numerical Recipes in Fortran*,

Second Edition. Cambridge University Press, Cambridge, 1992.

- [36] M. Abramowitz and I. A. Stegun, editors. *Handbook of Mathematical Functions with Formulas, Graphs, and Mathematical Tables.* Dover Publications, New York, 1964.
- [37] J. Fuchs. Harmonic-Inversion-Analyse exzeptioneller Punkte in Resonanzspektren. Bachelor thesis, Universität Stuttgart, 2013 (unpublished). URL: http://itp1.uni-stuttgart.de/publikationen/abschlussarbeiten/fuchs_bachelor_2013.pdf.
- [38] G. Wiebusch, J. Main, K. Krüger, H. Rottke, A. Holle, and K. H. Welge. Hydrogen atom in crossed magnetic and electric fields. *Phys. Rev. Lett.*, 62:2821–2824, 1989.
- [39] G. Raithel and H. Walther. Ionization energy of rubidium Rydberg atoms in strong crossed electric and magnetic fields. *Phys. Rev. A*, 49:1646–1665, 1994.
- [40] S. Freund, R. Ubert, E. Flöthmann, K. Welge, D. M. Wang, and J. B. Delos. Absorption and recurrence spectra of hydrogen in crossed electric and magnetic fields. *Phys. Rev. A*, 65:053408, 2002.
- [41] G. Stania and H. Walther. Quantum chaotic scattering in atomic physics: Ericson fluctuations in photoionization. *Phys. Rev. Lett.*, 95:194101, 2005.
- [42] J. Main and G. Wunner. Ericson fluctuations in the chaotic ionization of the hydrogen atom in crossed magnetic and electric fields. *Phys. Rev. Lett.*, 69:586–589, 1992.
- [43] C. Jaffé, D. Farrelly, and T. Uzer. Transition state theory without time-reversal symmetry: Chaotic ionization of the hydrogen atom. *Phys. Rev. Lett.*, 84:610–613, Jan 2000.
- [44] H. Cartarius, J. Main, and G. Wunner. Signatures of the classical transition state in atomic quantum spectra. *Phys. Rev. A*, 79:033412, 2009.
- [45] H. Cartarius, J. Main, T. Losch, and G. Wunner. Resonance wave functions located at the Stark saddle point. *Phys. Rev. A*, 81:063414, 2010.
- [46] T. N. Rescigno and V. McKoy. Rigorous method for computing photoabsorption cross sections from a basis-set expansion. *Phys. Rev. A*, 12:522–525, 1975.
- [47] W. P. Reinhardt. Complex coordinates in the theory of atomic and molecular structure and dynamics. *Ann. Rev. Phys. Chem.*, 33:223, 1982.
- [48] Y. K. Ho. The method of complex coordinate rotation and its applications to atomic collision processes. *Phys. Rep.*, 99:1–68, 1983.
- [49] J. Main and G. Wunner. Rydberg atoms in external fields as an example of open quantum systems with classical chaos. *J. Phys. B*, 27:2835–2848, 1994.
- [50] R. Lefebvre, O. Atabek, M. Šindelka, and N. Moiseyev. Resonance coalescence in molecular photodissociation. *Phys. Rev. Lett.*, 103:123003, 2009.
- [51] I. Gilary, A. A. Mailybaev, and N. Moiseyev. Time-asymmetric quantum-state-exchange mechanism. *Phys. Rev. A*, 88:010102(R), 2013.